Scattering of 14.7 MeV neutrons from ^{12}C and evidence for a new reaction channel

K. Gul, M. Anwar, M. Ahmad, S. M. Saleem, and Naeem A. Khan
Pakistan Institute of Nuclear Science and Technology, Nilore, Rawalpindi, Pakistan
(Received 23 February 1981)

Measurements of neutron scattering from carbon have been carried out for 14.7 MeV neutrons using associated particle and time-of-flight techniques. Angular distributions for the ground state, 4.43, and 7.65 MeV states have been measured in the laboratory angular range 30–130° and for the 9.63 MeV state in the range 30–70°. Double differential scattering cross sections have been obtained in the energy range 3–14 MeV. Monte Carlo simulation has been used to correct for multiple scattering including scattered flux attenuation. The integrated cross sections for 4.43 and 7.65 MeV states have been obtained as 214 ± 8 and 9.3 ± 1.6 mb, respectively. The present data have been compared with the published data. Evidence for a $^{12}C(n,\alpha)^{9}Be$ reaction populating the 6.76 MeV state and subsequently decaying by emission of a neutron has been observed for the first time. The presence of a neutron group of 5.6 MeV energy at backward angles has been discussed.

[NUCLEAR REACTIONS $^{12}C(n,n)$, $^{12}C(n,n')$, $^{12}C(n,\alpha n)$, $E = 14.7$ MeV; measured $\sigma(E,\theta)$, double differential scattering cross sections, integrated cross sections, natural target.]

I. INTRODUCTION

Measurements on neutron scattering by carbon have been reported by several authors[1–11] in the energy range 14.0–14.7 MeV. As there does not exist a resonance in the neutron total cross section of carbon in this energy range, the differential cross sections of various reaction channels should not show substantial variations over this energy interval. However, the reported data show variations which cannot be explained by the quoted errors. For example, the integrated cross section for the 4.43 MeV state reported by Haouat *et al.*[9] is about 40% less, and differential scattering cross sections for this state are systematically lower than reported previously below 60 degrees. Similarly, variations in the angular distributions for the 7.65 MeV state reported by different authors[12] are remarkably pronounced. In the present work we report measurements of 14.7 MeV neutrons scattering from carbon. We measured differential scattering cross sections for the ground state as well as for the 4.43 and 7.65 MeV states over the laboratory angular range 30–130 degrees. The angular distribution for the 9.63 MeV state was obtained over the angular range 30–70 degrees. The double differential scattering cross sections were derived over the outgoing energy range 3–14 MeV. The present measurements were compared with the published data. Evidence for the $^{12}C(n,\alpha)^{9}Be$ reaction populating the 6.76 MeV state in ^{9}Be and its subsequent decay by the emission of a neutron was observed for the first time. The presence of a neutron group of 5.6 MeV energy in the double differential scattering cross sections at backward angles is discussed.

II. EXPERIMENTAL PROCEDURE

The experiment was carried out using the PINSTECH neutron generator facility.[13] The energies of scattered neutrons were measured by the time-of-flight method based on the associated particle technique. The 14.7 MeV neutrons were generated through the $^{3}H(^{2}H,n)^{4}He$ reaction. The associated alpha particles were detected by a scintillator NE 810 viewed by an AVP 56 photomultiplier tube coupled to an Ortec 271 base which provided a timing signal to the stop channel of the time-to-pulse amplitude converter 467. The neutrons scattered

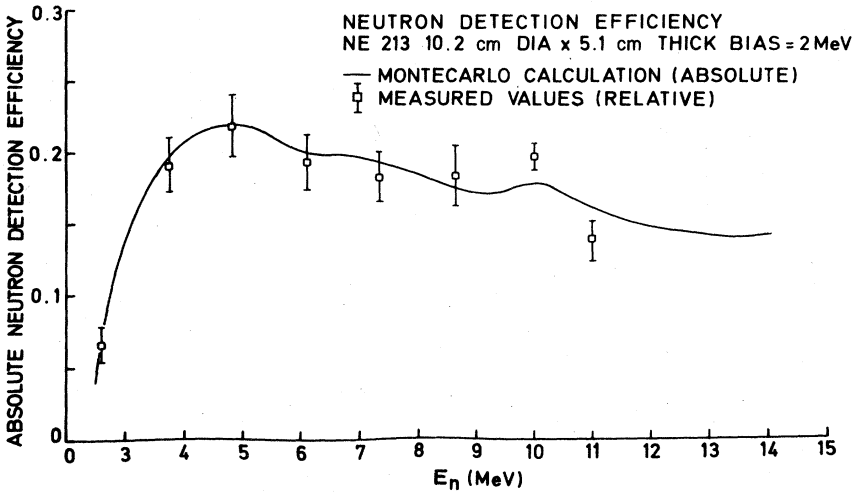

FIG. 1. The measured relative neutron detection efficiency of the neutron detector normalized to the absolute values of the efficiency computed by the Monte Carlo method.

from a 5.1 cm diameter $\times$ 5.1 cm long carbon sample placed at 13 cm from the neutron source were detected by a 10.2 cm diameter $\times$ 5.1 cm long NE 213 liquid scintillator viewed by an XP 1040 photomuliplier tube coupled to another Ortec 271 base which provided both a linear signal and a timing signal to the start channel of the time-to-pulse amplitude converter. A shadow bar was used to shield the main neutron detector from direct neutrons. In order to suppress the background due to gamma rays the neutron-gamma pulse shape discrimination technique was used by processing the linear pulse by an Ortec delay line amplifier 460 before feeding it into an Ortec pulse shape analyzer 458. The bias on the linear pulse from the neutron detector was set at about 2 MeV using a ^{22}Na source. It was ensured that the bias on the input pulses to the pulse shape analyzer was lower than the bias on the linear signal. The flux of neutrons was monitored with the help of a long counter and an independent time-of-flight system. The flight path of scattered neutrons was about 160 cm. The neutron spectra were obtained in the laboratory angular range 30—130 degrees. The relative detection efficiency of the neutron detector was measured as described in Refs. 13 and 14. The measured values of neutron detection efficiency are shown in Fig. 1, which also shows the absolute neutron detection efficiency computed with the help of the Rawal Monte Carlo code.[15]

III. DATA REDUCTION

A typical time-of-flight spectrum of neutrons scattered from carbon at 40 degrees is shown in Fig. 2. As the ground state and the first excited state at 4.43 MeV were not resolved completely, the areas under the two peaks were evaluated with the help of a computer code which gave a nonlinear least squares fit to a composite curve consisting of two Gaussian curves superimposed on a linear background. The code is based on subroutines contained in Ref. 16. Some of the subroutines were modified and extended for application to double peaks. The differential scattering cross sections were calculated from the expression

$$\frac{d\sigma(\theta)}{d\Omega} = \left[\frac{1}{A_f F}\frac{1}{N d\Omega_d}\right]\frac{Y(\theta)}{\epsilon(E)A_s},$$

where $d\Omega_d$ is the solid angle of the detector, A_f is the incident flux attenuation factor, F is the flux of neutrons at the scatterer, N is the total number of carbon atoms, $\epsilon(E)$ is the absolute neutron detection efficiency for a neutron of energy E, A_s is the scattered flux attenuation factor, and $Y(\theta)$ is the monitor normalized yield of neutrons at an angle θ which has been corrected for multiple scattering into the detector.

The factor within the parentheses was determined by normalizing the measured differential

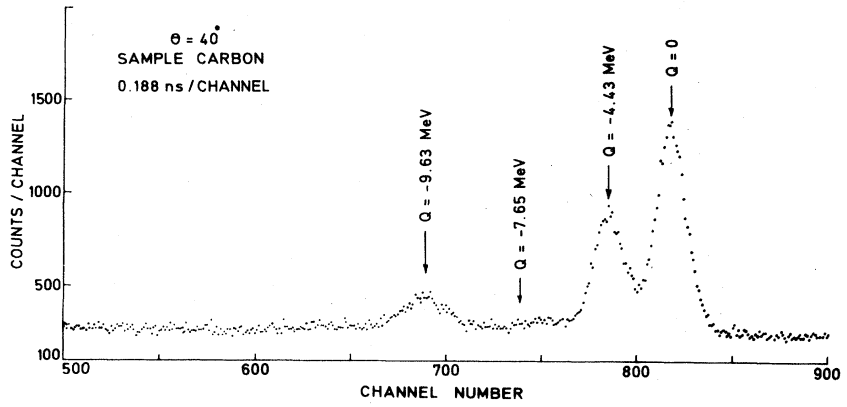

FIG. 2. Neutron time-of-flight spectrum of 14.7 MeV neutrons scattered from ^{12}C at 40° in the laboratory.

elastic scattering cross section at 70 degrees in the laboratory to 17.2 mb/sr reported by Haouat *et al.*[9] This value also agrees within given errors with the value computed from Legendre polynomial coefficients reported by Glasgow *et al.*[8] The computation of the multiple scattering correction including incident and scattered flux attenuation factors is described in the next section. The double differential scattering cross sections were computed with the help of a computer code developed for this purpose. The energy bins of 1 MeV in width were used for neutrons having energies above 8 MeV, while for lower energy neutrons the width was reduced to 0.5 MeV. The background for evaluation of double differential scattering cross sections was obtained through a least squares fit to a straight line consisting of data points spread over 150 channels in the neutron energy region where the neutron detector was biased off. The reduced chi-square values of the linear fit were always less than or equal to 1. This method of the background evaluation was adopted for the following reasons: (i) The background taken with the sample out was linear; slope depended on the intensity of the beam which could vary during runs. (ii) The general background was rather difficult to assess from a run with the sample out, particularly when a thick sample was being used, as it was not possible to simulate precisely the sample-in conditions.

IV. CORRECTIONS AND ERROR ANALYSIS

The multiple scattering correction consists of two parts: (i) The neutron flux scattered through single collisions in the direction of the detector gets scattered partially away through multiple scattering; this correction is called scattered flux attenuation. (ii) The neutron flux scattered through single collisions in directions other than that of the detector is partially directed into the detector through multiple collisions; the correction has been termed inscattering due to multiple scattering. In order to evaluate incident and scattered flux attenuation including the multiple inscattering correction and to correct for spurious peaks arising from multiple scattering,[17] a code was developed using the Monte Carlo simulation based on the forced collision technique. The relevant details of the technique may be found in the published literature.[15,17,18] The neutron flux was taken to be incident normally on the lateral surface of the cylindrical sample. Scattering from the 7.65 and 9.63 MeV states was assumed to be isotropic in the center of mass system. The published data[8,12] on the angular distributions of the ground state and the 4.43 MeV state were used for computing the scattering probabilities from these two states for neutrons of different energies. The data on total cross sections and total elastic cross sections for neutrons of different energies were taken from the IAEA ENDF/B-IV. The energy interval 0—15 MeV was divided into 30 bins each of a 500 keV width. The experimental angular resolution of ± 2 degrees was used. The incident and scattered flux attentuation factors for the neutrons of the ground state and the first three excited states at 4.43, 7.65, and 9.63 MeV were given by this code. As the scattered weight in energy regions other than the peaks was not statistically significant, the scattered flux attenuation factors for the evaluation of the double differential scattering cross sections were computed independently by allowing one forced col-

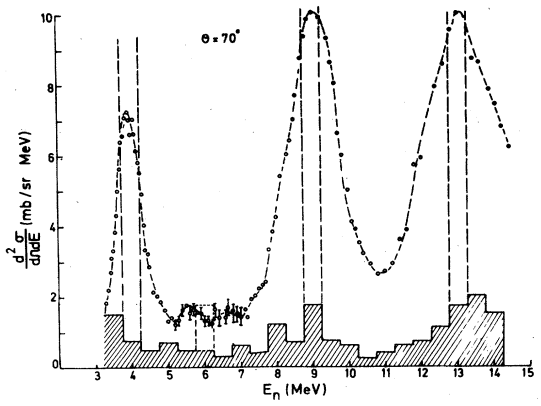

FIG. 3. The broken line through open circles represents double differential scattering cross sections at 70° corrected for scattered flux attenuation only. The hatched area represents the multiple inscattering correction.

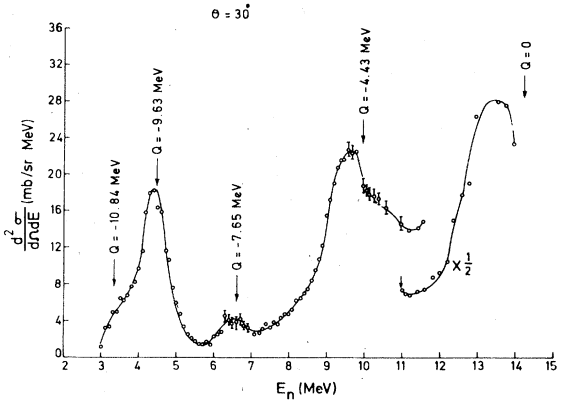

FIG. 4. The double differential scattering cross sections of carbon in the c.m. system at 30° for 14.7 MeV incident neutrons.

lision within the sample and measuring the attenuation of the transmitted weight from the point of collision. For the computation of multiple scattering corrections 60 000 incident trajectories were processed. The code was run on PDP-11/45. Figure 3 shows a typical illustration of an inscattering due to multiple scattering for double differential scattering cross sections at 70 degrees.

The following is the breakup of the error analysis in general: the flux normalization is less than 5%, the statistics is less than 1%, the multiple inscattering is less than 5%, the scattered flux attenuation is less than 4%, the dead time is less than 3%, the normalization is 10%, the neutron detection efficiency is less than 5%, and the overall error is less than 15%.

The statistical percentage of error on the double differential scattering cross sections was computed from the following expression:

$$\Delta\sigma = \frac{\sqrt{N}}{\Delta N} 100 ,$$

where N is the total number of neutrons including background and ΔN is the number of neutrons with the background subtracted. The errors shown on integrated cross sections are those given by fits.

V. RESULTS AND DISCUSSION

The measured values of double differential scattering cross sections are shown in Figs. 4—9.

The differential scattering cross section of a given state is obtained from $[d^2\sigma(\theta)]/d\Omega\, dE$ by integrating it with respect to energy. Therefore the values of the double differential scattering cross sections over a peak depend essentially on the width of a peak, which in turn depends on the energy resolution of the experiment. The only reported data on double differential scattering cross sections for carbon are those reported by Hermsdorf *et al.*[10] However, these measurements were carried out at a different energy resolution. The differential scattering cross sections for the ground state and the three excited states at 4.43, 7.65, and 9.63 MeV are shown in Figs. 10—13. No attempt has been made to fit the angular distributions with computations based on coupled channel considerations. Such calcula-

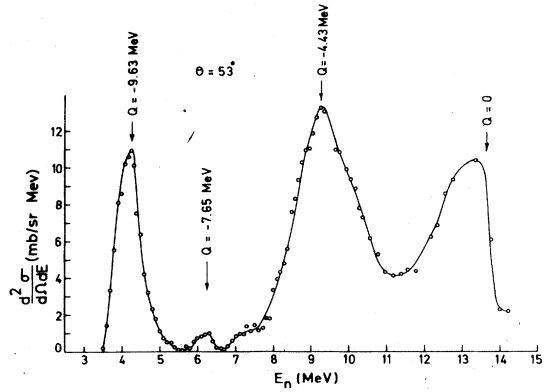

FIG. 5. The double differential scattering cross sections of carbon in the c.m. system at 53° for 14.7 MeV incident neutrons.

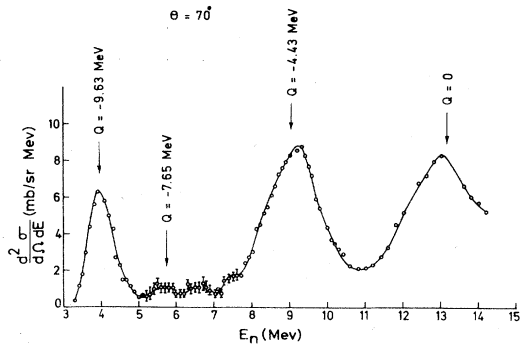

FIG. 6. The double differential scattering cross sections of carbon in the c.m. system at 70° for 14.7 MeV incident neutrons.

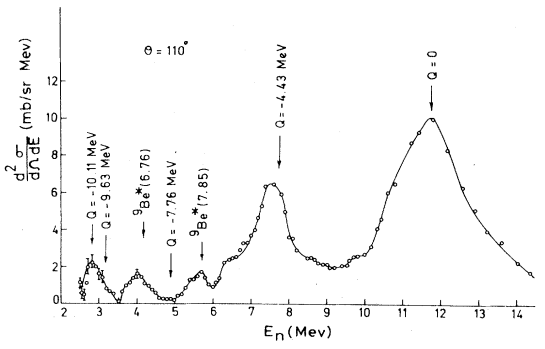

FIG. 8. The double differential scattering cross sections of carbon in the c.m. system at 110° for 14.7 MeV incident neutrons.

tions are reported in Refs. 6, 19, and 20. However, an interesting feature of these calculations is that the angular distributions of the excited states are fitted well only in the backward direction. The disagreement between the calculated and measured angular distributions increases considerably below 60 degrees. Over and above the neutron groups corresponding to the different levels of carbon, two more neutron groups have been seen clearly in the double differential scattering cross sections at backward angles. The origin of these neutron groups and results on the angular distributions are discussed in the following sections.

A. The ground state

The angular distribution of neutrons scattered from the ground state of carbon is shown in Fig. 10. Although the differential elastic scattering cross sections at this energy have been reported by several authors, only the data of Bouchez *et al.*,[2] Glasgow *et al.*,[8] and Haouat *et al.*[9] have been included for clarity of representation. Different sets of published[21] optical model potential parameters were tried for computation of differential elastic scattering cross sections, the total elastic cross section, and the reaction cross section using the optical model code[22] which is based on the methods of computation outlined in Ref. 23 and uses the Fox-Goodwin technique for the integration of the Schrödinger equation in the interior of the nucleus as described in Ref. 24. Only two sets gave overall good fits to the differential scattering cross sections. Both sets had been derived from the neutron scattering data on carbon taken at different energies.[9,25,26] These optical model potential parameters are given in Table I along with the corresponding computed values of total cross sections, total elastic cross sections, and reaction cross sections.

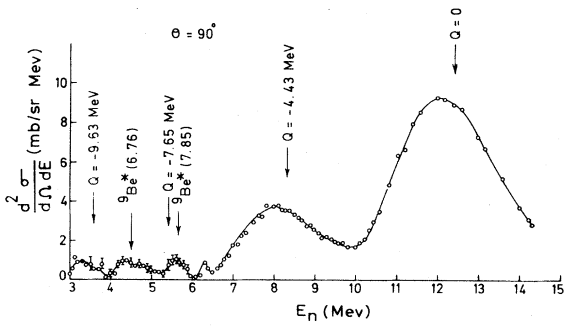

FIG. 7. The double differential scattering cross sections of carbon in the c.m. system at 90° for 14.7 MeV incident neutrons.

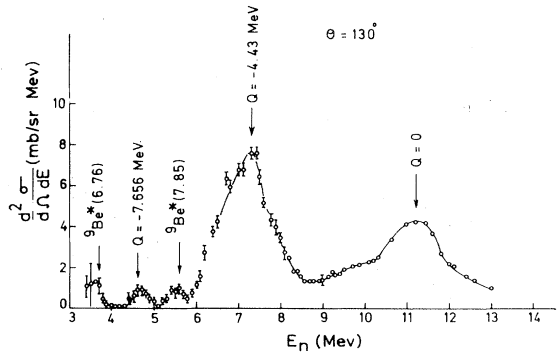

FIG. 9. The double differential scattering cross sections of carbon in the c.m. system at 130° for 14.7 MeV incident neutrons.

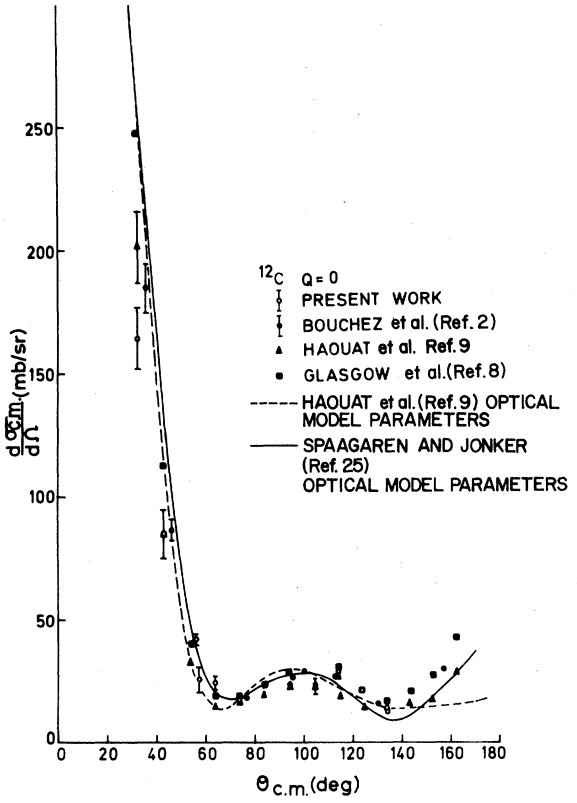

FIG. 10. The differential scattering cross sections of the ground state of ^{12}C and its comparison with optical model calculations and published data.

B. The 4.43 MeV state

Our data on the differential scattering cross sections for the 4.43 MeV state are shown in Fig. 11. The results are compared with the data of Bouchez *et al.*,[2] Haouat *et al.*,[9] and Glasgow *et al.*[8] The present data agrees with the data of Bouchez *et al.*[9] below 60 degrees, where it does not agree with the results of Haouat *et al.*[9] and Glasgow *et al.*,[8] which data also do not agree with one another in the forward direction. In order to obtain an integrated cross section for this state a least-squares fit to the sum of the Legendre polynomials of different orders was done with the following Legendre polynomial coefficients:

$$A_0 = 17.20 \pm 0.65 ,$$

$$A_1 = 15.34 \pm 1.06 ,$$

$$A_2 = 25.40 \pm 1.35 .$$

A value of 214 ± 8 mb was obtained for the inelastic scattering cross section to the 4.43 MeV state. An extensive comparison of the integrated cross section to this state may be found in Ref. 27.

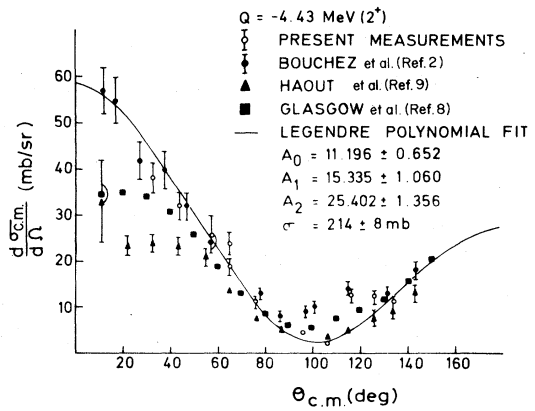

FIG. 11. The differential scattering cross sections of the 4.43 MeV state in ^{12}C.

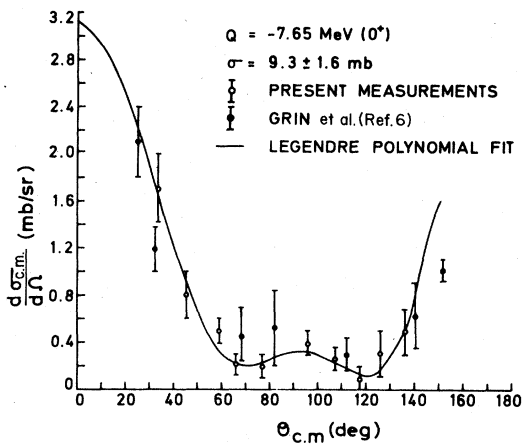

FIG. 12. The differential scattering cross sections of the 7.65 MeV state in ^{12}C.

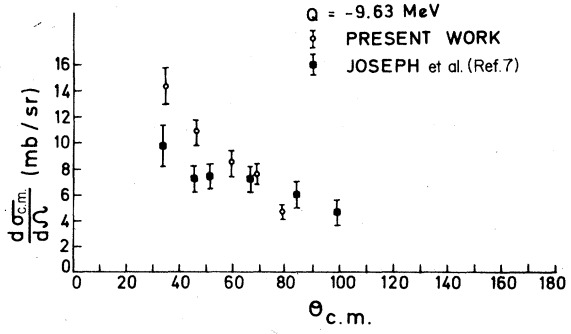

FIG. 13. The differential scattering cross sections of the 9.63 MeV state in ^{12}C.

TABLE I. Two sets of optical model potential parameters used in computing cross sections for the ground state of ^{12}C. The references refer to the optical model parameters contained in each line. The computed cross sections have been obtained using the listed parameters.

V (MeV)	r_V (fm)	a_V (fm)	w_D (MeV)	RWD (fm)	A_{W_D} (fm)	U_{so} (MeV)	$R_{V_{so}}$ (fm)	a_{so} (fm)	σ_r (mb)	σ_e (mb)	σ_t (mb)
46.49	1.28	0.39	8.88	0.86	0.39	4.39	1.28	0.39	434	834	1268[a]
50.8	1.25	0.36	7.86	1.25	0.27	6.15	1.25	0.36	415	824	1239[b]

[a]From Ref. 25.
[b]From Ref. 9.

C. The 7.65 MeV state

The angular distribution of neutrons scattered from the 7.65 MeV state are shown in Fig. 12 and compared with the data of Grin *et al.*[6] The neutron groups of this state overlap with a group of neutrons of rather unknown origin occurring at about 5.6 MeV at 70, 90, and 100 degrees. There could be a contribution of about 0.2 mb/sr from this group at these angles which has not been subtracted. The angular distribution was fitted with a sum of Legendre polynomials and the best fit was obtained with the following coefficients:

$$A_0 = 0.743 \pm 0.135 ,$$
$$A_1 = 0.078 \pm 0.413 ,$$
$$A_2 = 1.672 \pm 0.396 ,$$
$$A_3 = -0.211 \pm 0.620 ,$$
$$A_4 = 1.094 \pm 0.38 ,$$
$$A_5 = -0.307 \pm 0.469 .$$

A value of 9.3 ± 1.6 mb was obtained for the integrated cross section of this state.

D. The 9.63 MeV state

The angular distribution for the 9.63 MeV state is shown in Fig. 13, which also shows its comparison with the published data. The present results on the integrated cross sections for levels in ^{12}C except for the 9.63 MeV state are listed in Table II and compared with the published data.

E. The origin of extra neutron groups

Apart from the neutron groups corresponding to the various states of carbon, two more neutron groups have been observed in the double differential scattering cross sections. A group of neutrons of 5.6 MeV in energy has been very clearly seen at 70, 90, 100, 110, and 120 degrees which partially over-

TABLE II. Summary of the measured integrated scattering cross sections of the various states of ^{12}C and their comparison with the published data.

	Present	Haouat *et al.* (Ref. 7)	Glasgow *et al.* (Ref. 8)	Bouchez *et al.* (Ref. 2)	Grin *et al.* (Ref. 6)	Clark Cross
Ground state	830 ± 15[a]	730	887 ± 52	810 ± 40	775 ± 35	730 ± 70
4.43 MeV	214 ± 8	146.4 ± 8	202 ± 8.8	215 ± 40	215 ± 15	209 ± 20
7.65 MeV	9.3 ± 1.6			16 ± 10	8.5 ± 2	

[a]Average value of the elastic scattering cross-section computed from the optical model parameters containing in Table I.

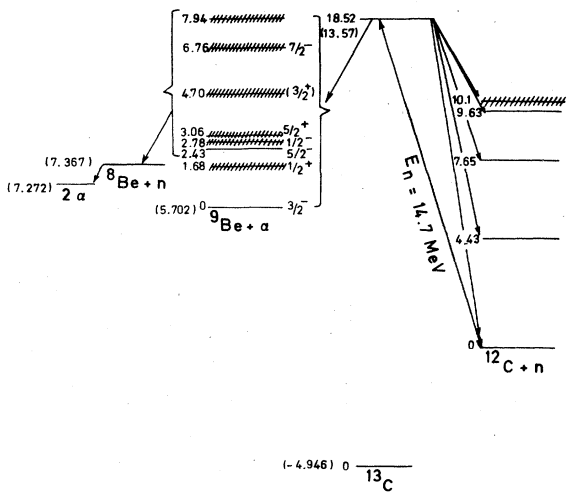

FIG. 14. Energy levels involved in $^{12}C(n,n')^{12}C$ and $^{12}C(n,\alpha)^{9}Be^{*}$, $^{9}Be^{*} \rightarrow {}^{8}Be + n$ reactions.

laps with the group of neutrons of the 7.65 MeV state at the first three angles. This group of neutrons shows almost no energy variation with the scattering angle. The second neutron group has energy between 4 and 5 MeV and has been observed in the angular range 70—130 degrees. In contrast to the first neutron group, the second neutron group shows an energy variation with the scattering angle. As may be seen from Fig. 14, the compound nucleus, besides its decay to the various levels of ^{12}C, can also decay to the different stats of ^{9}Be through emission of an alpha particle. The levels in ^{9}Be above the 1.67 MeV state can decay by emission of a neutron to ^{8}Be, which can give rise to extra neutron groups. The neutron group which shows energy variation with the scattering angle has been attributed to the decay of $^{9}Be^{*}$ (6.76 MeV) nuclei through emission of a neutron. The $^{9}Be^{*}$ (6.76) nuclei move in a cone of angular width of about 41° in the forward direction. It has been reported that the n-α reaction on carbon proceeds mainly through the direct reaction mechanism,[28,29] and thus alpha particles could be emitted predominantly in the forward or backward direction. In both cases $^{9}Be^{*}$ (6.76) nuclei are emitted in the forward direction with the two limiting energies of 0.091 and 2.15 MeV in the zero direction. The computed energies of neutrons in backward directions emitted from $^{9}Be^{*}$ (6.76 MeV) moving with these two limiting energies are shown in Table III. The observed energies of neutron groups lie within these computed values and agree with the average values at these angles. The differential scattering cross sections for this neutron group are given in Table IV.

The presence of the 5.6 MeV neutron group is rather difficult to explain. It is of interest to note that a neutron group of about this energy is also present in the double differential scattering cross sections for carbon reported by Hermsdorf *et al.*[10] A neutron group of this energy can arise from the decay of stationary nuclei of $^{9}Be^{*}$ (7.85 MeV). The existence of a 7.94 MeV state has been reported.[30] However, the reported width of this state is about 1 MeV and does not correspond to enough long life to enable $^{9}Be^{*}$ (7.94) nuclei to lose their 0.78 MeV energy and come to rest before emitting a neutron.

TABLE III. The computed values for the energies of neutrons corresponding to the two values of kinetic energy of $^{9}Be^{*}$ (6.76) nuclei moving in the forward direction and their comparison with the observed energy values.

θ_{lab} (degrees)	E_{n1} (MeV)	E_{n2} (MeV)	$\overline{E}_n$ (MeV)	E_{obs} (MeV)
90	4.52	4.29	4.41	4.5 ± 0.2
100	4.45	3.95	4.20	4.3 ± 0.2
110	4.38	3.65	4.02	4.1 ± 0.2
120	4.31	3.39	3.85	4.0 ± 0.2
130	4.25	3.17	3.71	3.7 ± 0.2

TABLE IV. The differential scattering cross sections of neutrons emitted from ^{9}Be* (6.76) populated through the n-α reaction on ^{12}C for the 14.7 MeV incident neutrons.

θ_{lab}	$\frac{d\sigma_{c.m.}}{d\Omega}$ (mb/sr)
90	0.4 ± 0.2
100	0.3 ± 0.2
110	0.8 ± 0.2
120	0.2 ± 0.1

F. An estimate of the $n - 3\alpha$ reaction cross section

Assuming that energy levels above 7.65 MeV decay by particle emission, the reaction cross section excluding that for the n-3α reaction is the sum of the scattering cross sections for 4.43 and 7.65 MeV states and the cross section for the n-α reaction to the ground state of ^{9}Be. This comes to about 292 mb by taking 69 mb for the n-α reaction cross section to the ground state of ^{9}Be. The average of the two reaction cross sections listed in Table I then gives 133 mb for the n-3α reaction cross section.

VI. CONCLUSION

Angular distributions of the ground state and the first three excited states in ^{12}C have been measured for 14.7 MeV incident neutrons and the data were compared with the published results. Double differential scattering cross sections were obtained and two new neutron groups were observed. The existence of one of the group has been explained, while that of the other group occurring at 5.6 MeV cannot be explained properly. The importance of the presentation of neutron spectra in the form of double differential scattering cross sections in revealing the presence of weak neutron groups which get masked in time-of-flight spectra has been established.

ACKNOWLEDGMENTS

The authors thank the IAEA for providing information from ENDF/B-IV on ^{12}C. They are also thankful to the scientific staff of the Neutron Generator for their help during the experiment.

[1]R. L. Clarke and W. G. Cross, Nucl. Phys. 53, 177 (1964).
[2]R. Bouchez, J. Duclos, and P. Perrin, Nucl. Phys. 43, 628 (1963).
[3]J. Rethmeier, C. C. Jonker, M. Rodenberg, J. Hovenier, and D. Van der Meulem, Nucl. Phys. 38, 322 (1962).
[4]T. Tesch, Nucl. Phys. 37, 412 (1962).
[5]M. P. Nakada, J. D. Anderson, C. C. Gardner, and C. Wong, Phys. Rev. 110, 1439 (1958).
[6]G. A. Grin, B. Vaucher, J. C. Alder, and C. Joseph, Helv. Phys. Acta 42, 990 (1969).
[7]C. Joseph, G. A. Grin, J. C. Alder, and B. Vaucher, Helv. Phys. Acta 40, 693 (1967).
[8]D. W. Glasgow, F. O. Purser, H. Hogue, J. C. Clement, K. Stelzer, G. Mack, J. R. Boyce, D. H. Epperson, S. G. Buccino, P. W. Lisowski, S. G. Glendinning, E. G. Bilpuch, H. W. Newson, and C. R. Gould, Nucl. Sci. Eng. 61, 521 (1976).
[9]G. Haouat, J. Lachkar, J. Siguad, Y. Patin, and F. Cocu, Nucl. Sci. Eng. 65, 331 (1978).
[10]D. Hermsdorf, A. Meister, S. Sassonoff, D. Seeliger, K. Siedel, and F. Shahin, Central Institute of Nuclear Physics Rossendorf Report No. ZfK-277(u), IAEA INDC Report No. INDC(GDR)-2/L, 1975.
[11]B. Antolkovic and Z. Dolenec, Nucl. Phys. A237, 235 (1975).
[12]D. I. Garber, L. G. Stromberg, M. D. Goldberg, D. E. Cullen, and V. M. May, BNL Report 400 1, 1970.
[13]K. Gul, A. Waheed, M. Ahmad, M. Saleem, and Naeem A. Khan, J. Phys. G 5, 1107 (1979).
[14]A. Waheed, K. Gul, M. Ahmad, S. M. Saleem, and Naeem A. Khan, Nucleus (Pakistan) 15, 3 (1978).
[15]K. Gul, Nucl. Instrum. Methods 176, 549 (1980).
[16]Philip R. Bevington, *Data Reduction and Error Analysis for the Physical Sciences* (McGraw-Hill, New York, 1969).
[17]J. B. Parker, J. H. Towle, D. Sams, W. B. Gilboy, A. D. Purnell, and H. J. Stevens, Nucl. Instrum. Methods 30, 77 (1964).
[18]E. D. Cashwell and C. J. Everett, *Practical Manual on the Monte Carlo Method for Random Walk Problems* (Pergamon, London, 1959).
[19]G. A. Grin, C. Joseph, C. Y. Wong, and T. Tamura, Phys. Lett. 25B, 387 (1967).
[20]M. Thumm, H. Lesiecki, G. Mertens, K. Schmidt, and G. Mack, Nucl. Phys. A344, 446 (1980).
[21]C. M. Perey and F. G. Perey, At. Data Nucl. Data Tables 17, 1 (1976).

[22]K. Gul (unpublished).
[23]B. Buck, R. N. Maddison, and P. E. Hodgson, Philos. Mag. 5, 1187 (1960).
[24]M. A. Melkanoff, T. Swada, and J. Raynal, Methods Comput. Phys. 6, 1 (1966).
[25]D. Spaagaren and C. C. Jonker, Nucl. Phys. A161, 354 (1971).
[26]B. A. Watson, P. P. Singh, and R. E. Segel, Phys. Rev. 182, 977 (1969).
[27]J. Lachkar, F. Cocu, G. Haouat, P. L. Floch, Y. Patin, and J. Siguad, Institute de Bruyeres-le-Chatel Report No. NEANDC (E) 168 "L", 1975.
[28]M. L. Chatterjee and B. Sen, Nucl. Phys. 51, 583 (1964).
[29]R. A. Al-Kital and R. A. Peck, Jr., Phys. Rev. 130, 1500 (1963).
[30]F. Ajzenberg-Selove, Nucl. Phys. A320, (1980).